

Nagaoka ferromagnetism in doped Hubbard models in optical lattices

Rhine Samajdar^{1,2} and R. N. Bhatt^{1,3}

¹*Department of Physics, Princeton University, Princeton, NJ 08544, USA*

²*Princeton Center for Theoretical Science, Princeton University, Princeton, NJ 08544, USA*

³*Department of Electrical and Computer Engineering,*

Princeton University, Princeton, NJ 08544, USA

(Dated: May 11, 2023)

The search for ferromagnetism in the Hubbard model has been a problem of outstanding interest since Nagaoka’s original proposal in 1966. Recent advances in quantum simulation have today enabled the study of tunable doped Hubbard models in ultracold atomic systems. Here, we examine a realistic variant of such a model wherein any second electron on a single lattice site is weakly bound compared to the first one. Employing large-scale density-matrix renormalization group calculations, we establish the existence of high-spin ground states on square and triangular lattices, analyze the microscopic mechanisms behind their origin, and investigate the interplay between ferromagnetism and other competing orders, such as stripes. Our results also explain—and shed new light on—the intriguing observations of ferromagnetic correlations in recent optical-lattice experiments.

Introduction.—The Hubbard model is a paradigmatic model of modern condensed matter physics that is widely used to study a variety of strongly correlated systems [1]. It describes electrons hopping on a lattice with a tunneling amplitude t and interacting via an onsite potential U . Despite its seeming simplicity, this model harbors tremendously rich physics [2, 3] and is often believed to underlie a host of materials, including the high-temperature cuprate superconductors [4].

Over the last decade, ultracold atoms trapped in optical lattices have emerged as an exceptionally promising and versatile platform for realizing Hubbard models [5, 6]. Recently, a number of such cold-atom experiments [7–11] have demonstrated the existence of long-range antiferromagnetic order in two dimensions. Antiferromagnetism arises quite commonly in the Hubbard model, the magnetic excitations of which are described by a Heisenberg model of spins at half filling (one electron per site) [12] or, more generally, by a so-called t - J model [13] in the doped system. In both cases, the electron-electron interactions give rise to a superexchange $J \sim -t^2/U$ [14], which favors antialignment of spins.

Away from half filling, the kinetic term of the model can actually favor *ferromagnetism*, which is much rarer in the phase diagram. In 1966, Nagaoka [15] rigorously proved that for $U/t = \infty$, the ground state of the Hubbard model on a bipartite lattice with a single hole away from half filling is ferromagnetic [16]. For finite U/t , however, in the thermodynamic limit, the ground state is antiferromagnetic at half filling in all integer dimensions $d > 1$ [17]. Since then, a number of studies have sought to determine if and when “Nagaoka ferromagnetism” is obtained for finite U/t [18–20] or practically relevant dopings [21–25] with varying degrees of success. In the absence of a conclusive answer, various routes towards *inducing* ferromagnetism in modified Hubbard models have been explored, including the introduction of multiple orbitals, nearest-neighbour Coulomb repulsion, longer-range hop-

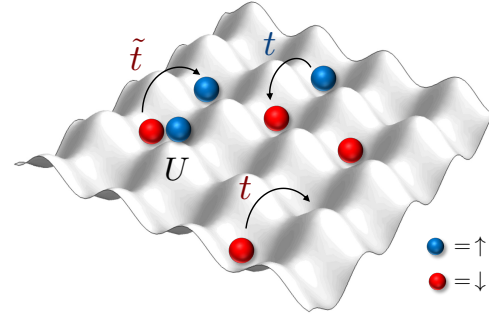


Figure 1. A schematic illustration of the extended Hubbard model described in Eq. (1). Fermions hop on an optical lattice with an onsite repulsive interaction U and a tunneling amplitude t , which is enhanced to \tilde{t} for a hopping process from a doubly occupied site to an already singly occupied site.

pings, or dispersionless (“flat”) bands in the spectrum [26–28].

In this work, we investigate a much simpler variant of the Hubbard model—inspired by studies of hydrogenic donors in semiconductors [29–31]—which can be realized in today’s optical lattice setups. In particular, we consider a situation in which the second electron on any site of the lattice is much more weakly bound than the first. A Hamiltonian which captures this essential physics of electron doping away from half filling within the Hilbert space of the Hubbard model is given by [30]

$$H = - \sum_{\langle i,j \rangle, \sigma} \left(t(n_i, n_j) c_{i\sigma}^\dagger c_{j\sigma} + \text{h.c.} \right) + U \sum_i n_{i\uparrow} n_{i\downarrow}, \quad (1)$$

where $n_{i,\sigma} \equiv c_{i,\sigma}^\dagger c_{i,\sigma}$ denotes the number operator on site i , $n_i = n_{i,\uparrow} + n_{i,\downarrow}$ is the total occupation of site i , and the occupation-dependent nearest-neighbor hopping is given by $t(n_i, n_j) = \tilde{t}$ if $n_i = 1, n_j = 2$ and $t(n_i, n_j) = t$ otherwise. This enhanced hopping (for electron-doped systems) favors the formation of a locally ferromagnetic configuration of spins around the charge, thus yielding a polaronic type of ferromagnetism in the large- U/t limit.

Studying this extended Hubbard model in the strong-correlation limit $U \gg t$ using large-scale density-matrix renormalization group (DMRG) [32] calculations, we discover extended regions of ferromagnetic order in the phase diagram on square and triangular lattices. We further characterize its intrinsic connection to geometric frustration and discuss its competition with other proximate orders, such as striped phases. Note that our analysis also encompasses the standard Hubbard model, which Eq. (1) reduces to for $\tilde{t}=t$. Our results thus directly address the recent experiments by Xu *et al.* [33] observing ferromagnetism in a frustrated Fermi-Hubbard magnet and account for the origins thereof.

Square lattice.—Our search for elusive ferromagnetism begins with the square lattice. At half filling, the ground state of the square-lattice Hubbard model is known to be a Mott insulator with antiferromagnetic Néel order for all values of $U/t > 0$ due to the perfect nesting of the noninteracting Fermi surface. As the doping (either electron or hole) is increased, one expects a transition to a ferromagnetic ground state for sufficiently large U/t . However, note that for $\tilde{t} \neq t$, the particle-hole symmetry possessed by the standard Hubbard model on bipartite lattices is lost. In fact, exact diagonalization calculations on small clusters [29, 30] have previously identified that high-spin ground states are obtained at much lower values of U/t for electron doping than for hole doping. Therefore, we choose to focus on the electron-doped case hereafter.

We systematically probe the ground states of the Hamiltonian (1) using DMRG. In order to study two-dimensional systems with DMRG [34], we work on cylinders of N sites, with dimensions $L_x \times L_y$ (in units of the lattice spacing a) and open (periodic) boundary conditions along the \hat{x} (\hat{y}) direction. Using a bond dimension of up to $\chi = 4800$, we ensure the convergence of our results to a truncation error $< 10^{-7}$ throughout.

Figure 2 illustrates the ground states thus obtained at $\tilde{t}/t = 4$ for two representative values of U/t , at a doping fraction of $\delta = 1/12$ above half filling (which we find to be optimal for ferromagnetism). At $U = 9\tilde{t}$, one clearly observes a saturated ferromagnetic ground state [Fig. 2(b)], as evidenced by the uniform spin-density profile in real space with $\langle S_i^z \rangle$ attaining its maximum possible value (the spin operator is defined as $\mathbf{S}_i = c_{i\alpha}^\dagger \boldsymbol{\sigma}_{\alpha\beta} c_{i\beta}$). The long-ranged ferromagnetic correlations in this fully polarized state are also reflected in the static structure factor $\mathcal{S}(\mathbf{q}) = \sum_{i,j} \langle \mathbf{S}_i \cdot \mathbf{S}_j \rangle / N$, shown in Fig. 2(d), which only exhibits a single peak at $\mathbf{q} = 0$ in the Brillouin zone.

Interestingly, our calculations uncover a competing ground state with stripe order, i.e., unidirectional charge and spin density modulations [35–37]. An example of this inhomogeneous striped state, which breaks translational and rotational symmetries, is displayed in Fig. 2 (a) and (c) in real and Fourier space, respectively, for $U = 6\tilde{t}$. The static structure factor now shows prominent peaks at $(\pm\pi/3, 0)$ indicating a period-6 modulation of the spin

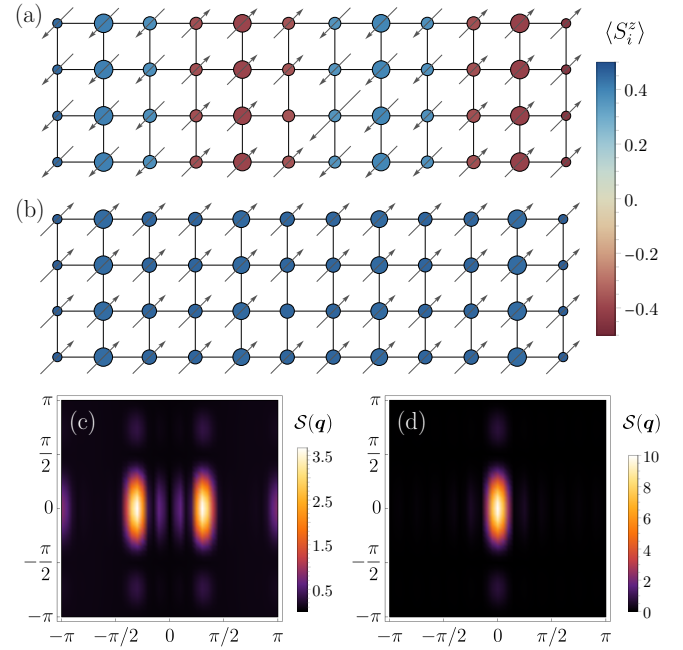


Figure 2. Ground states of the extended Hubbard model (1) at $\tilde{t}/t = 4$ for (a) $U = 6\tilde{t}$ and (b) $U = 9\tilde{t}$. The color of each circle conveys the onsite magnetization $\langle S_i^z \rangle$ while its diameter is proportional to the charge density $\langle n_i \rangle$. The length of the arrows is proportional to the amplitude of the spin correlation $\langle \mathbf{S}_0 \cdot \mathbf{S}_i \rangle$ with respect to the central site, indexed 0 (arrow-free). The directions of the arrows encode the sign of $\langle \mathbf{S}_0 \cdot \mathbf{S}_i \rangle$ with arrows pointing northeast (southwest) indicating positive (negative) correlations. (c,d) The static spin structure factors corresponding to the states in (a,b), respectively.

density along the nonperiodic direction, which accompanies a period-3 modulation of the charge density. Across a wide range of L_x (Fig. 3), we find that the stripes are *filled* and commensurate with the doping, accommodating exactly one excess electron per unit cell of 12 sites for $\delta = 1/12$. Such stripes have been experimentally observed in certain cuprates [38, 39] and identifying their fingerprints in the hole-doped Hubbard model has been the subject of intense numerical effort [40–49]. In our case, the origin of the stripes can be understood as follows. Consider a state with stripes of linear width ℓ . Relative to the uniform ferromagnet, the increase in the electrons' kinetic energy will be $E_K \sim (\delta N) \tilde{t} / (\ell L_y)$ while the decrease in interaction energy due to the antiferromagnetic exchange across the domain walls is $E_J \sim -J N / \ell$. The competition of these two energy scales decides between ferromagnetic and stripe orders, with the former eventually prevailing at large enough U/t (as $J \sim -t^2/U$).

Having established the existence of the Nagaoka state, we now turn to characterizing its extent and stability. To do so, we define an order parameter, namely, the average magnetization $m = |\sum_i \langle S_i^z \rangle / N| = |\sum_i \langle n_{i,\uparrow} - n_{i,\downarrow} \rangle / (2N)|$, which is plotted in Fig. 3(a) as a function of U/t for three different system sizes. The onset of ferromagnetism is apparent as a sharp increase in m at $U/t \sim 30$, wherafter m

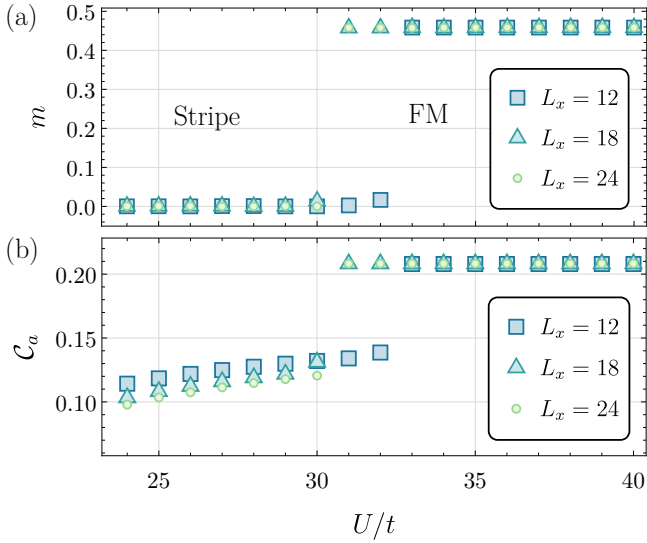


Figure 3. (a) The average magnetization m and (b) the radially averaged nearest-neighbor correlator C_a at $\tilde{t}/t = 4$ for three width-4 cylinders of different lengths, showing the transition from the striped to the ferromagnetic ground state on the square lattice.

quickly saturates to a system-size-independent value [50]. Importantly, the pinning of the order parameter to this maximal value over an extended range of U/t demonstrates that the ferromagnet is also stable against spin flips (*unlike* the original single-hole-doped Nagaoka state [17]). Intuitively, this is because the gain of band energy due to a single flipped spin never exceeds the concomitant cost from the onsite repulsion, and hence, we do not observe a partially polarized ferromagnetic state.

Owing to the $SU(2)$ spin-rotation symmetry of the Hubbard model, the quantum ferromagnet can be polarized along *any* axis and not necessarily \hat{z} . Hence, a better metric to quantify the ferromagnetic order is the normalized averaged two-point correlation function $C_d = \sum_{\langle i,j \rangle, ||\mathbf{r}_i - \mathbf{r}_j||=d} \langle \mathbf{S}_i \cdot \mathbf{S}_j \rangle / \mathcal{N}_b$, where the sum runs over \mathcal{N}_b unordered pairs of sites $\langle i,j \rangle$ separated by a distance d . In particular, Fig. 3(b) shows the nearest-neighbor correlator C_a , revealing a qualitatively similar behavior to m across the stripe–ferromagnet transition. Since this quantum phase transition occurs between two different magnetically ordered symmetry-breaking states, by Landau theory, we expect it to be first-order; this is indeed borne out by the sudden jump in m, C_a as U/t is varied.

Lastly, we note that decreasing (increasing) \tilde{t}/t increases (decreases) the minimal U/t required for a fully polarized ground state. For instance, in stark contrast to Fig. 3, we do not detect any Nagaoka ferromagnet up to $U/t = 50$ for $\tilde{t}/t = 2$ on the same cylinders. This is because ferromagnetism is driven by the relative kinetic energy gain of a delocalized electron in a background of aligned spins vis-à-vis the background being in an anti-

ferromagnetic or random configuration, and this gain is reduced by a smaller hopping amplitude.

Triangular lattices.—Our observation of electron-hole asymmetry aiding the formation of ferromagnetic states or domains on square arrays raises the natural question of whether similar behavior occurs on nonbipartite lattices, which innately lack electron-hole symmetry even for $\tilde{t} = t$. Mattis [51] established two general conditions regarding the geometric constraints required to host Nagaoka ferromagnetism: the underlying lattice should have loops, and different paths of particles or holes around such loops should interfere constructively. On the unfrustrated square lattice, the shortest such path is a cluster of four sites, which leads to a hopping amplitude $\sim t^4$. However, it is the nonbipartite triangular lattice which exhibits the *shortest* possible loop length of three. Consequently, the loop-hopping amplitude is proportional to t^3 and changes sign when t does (which is equivalent to exchanging electron and hole doping), so we expect to find ferromagnetism only for $\delta > 0$.

The simplest geometry endowed with such loops is a two-leg triangular ladder, which we now investigate. Earlier dynamical mean-field theory (DMFT) calculations on the Hubbard ($\tilde{t} = t$) model found the region of ferromagnetism in parameter space to be maximized for an electron doping concentration of $\delta = 0.5$ [52]. While DMFT is exact only in infinite dimensions, we use this filling fraction as a starting point for the extended Hubbard model (1) as well. Figure 4(a) sketches the ground state of the Hamiltonian on a 30-site-long two-leg ladder for $\tilde{t}/t = 4$, $U = 0.5\tilde{t}$. Even for this rather small value of U/t , we unambiguously observe large-scale ferromagnetic order across the entire system, characterized by a saturated magnetization of $m = 0.25$ with a standard deviation of 0.015. The mechanism behind the emergence of this Nagaoka state is the presence of an asymmetric density of states with a peak at the appropriate band edge (lower edge of the upper Hubbard band in this case) since a large density of states at the Fermi level, E_F , lowers the kinetic cost associated with filling additional single-particle electronic states, thereby enabling the large U (that favors spin alignment) to dominate [53–55].

Motivated by this finding, we systematically explore the dependence of ferromagnetism on the Hamiltonian’s parameters by constructing a phase diagram based on the magnetization m [Fig. 4(b)]. We see that increasing \tilde{t}/t results in a dramatic reduction in the minimal U/t needed for the development of ferromagnetic order. To probe the robustness of this behavior, we consider two cuts through this phase diagram, for three ladders of varying lengths, and inspect the two-point correlator C_a . For the Hubbard limit $\tilde{t}/t = 1$ [Fig. 4(c)], we find that the correlations in the ground state (which is believed to be a Curie-Weiss metal for low U/t [52]) remain negative till $U/t \sim 40$ and turn weakly ferromagnetic thereafter. On the contrary, for $\tilde{t}/t = 4$ [Fig. 4(d)], this transition occurs for a nearly

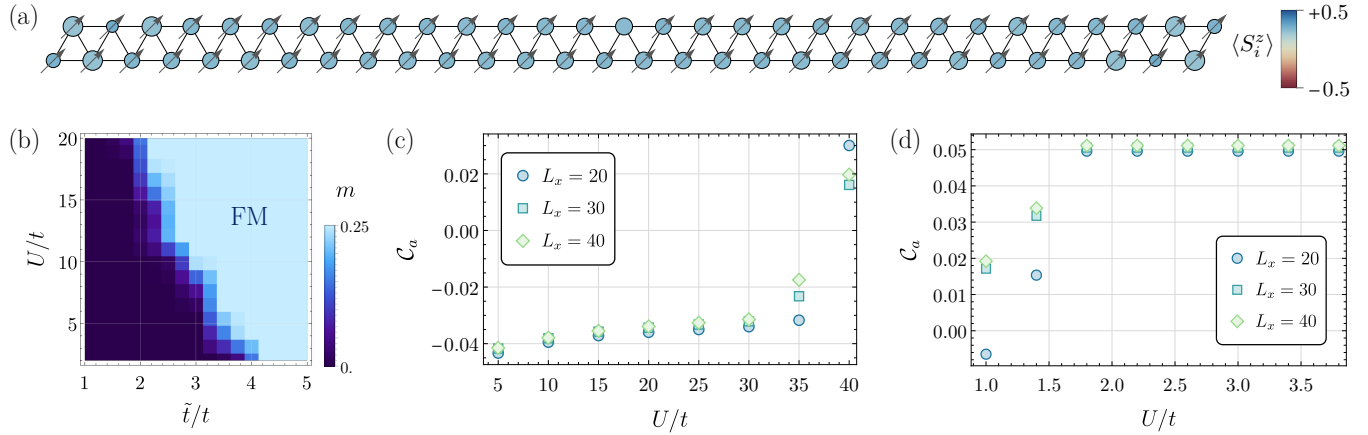


Figure 4. (a) Ground state obtained on a triangular two-leg ladder for $\tilde{t}/t = 4$, $U = 0.5\tilde{t}$ (drawn using the same conventions as in Fig. 2), displaying macroscopic long-ranged ferromagnetic correlations. (b) Phase diagram of a $L_x = 20$ ladder, as chalked out by the magnetization m , showing the extent of the Nagaoka state (FM). (c,d) The nearest-neighbor correlator C_a for ladders of three different lengths, demonstrating the development of ferromagnetism as a function of U/t along the cuts (c) $\tilde{t}/t = 1$ (the Hubbard limit) and (d) $\tilde{t}/t = 4$. All calculations presented here are for an electron doping concentration of $\delta = 0.5$.

twentyfold smaller U/t , irrespective of system size.

Another key property conveyed by Fig. 4 is the significant reduction of the threshold U/t for the triangular ladder as compared to the square lattice. Classically, one might suspect this to be an effect of the geometric frustration, which is deleterious to competing antiferromagnetic orders and leads to their suppression. Such a reasoning, however, may break down due to subtle quantum effects; for example, antiferromagnetism can actually be *enhanced* on the triangular lattice by a single hole [56]. Instead, Nagaoka ferromagnetism on the triangular lattice can be better understood as a consequence of geometrical frustration of the kinetic energy—a strictly quantum-mechanical effect stemming from quantum interference [52]. A quantitative measure of such kinetic energy frustration is given by $f \equiv W/(2z|t|)$, where W is the bandwidth and z is the coordination number [57], with smaller ratios indicating stronger frustration. The kinetic frustration of even a single triangular cluster results in lowering f below the unfrustrated value of $f = 1$ for the square lattice [52].

While our results on the square lattice and the triangular ladder manifest the presence of a Nagaoka state when assisted by $\tilde{t} > t$, it is only natural to ask if there are conditions under which ferromagnetism occurs for moderate values of U/t even in the Hubbard limit (i.e., $\tilde{t} = t$). To answer this question, we now consider the triangular-lattice Hubbard model. In this case, the noninteracting problem has a bandwidth of $9t$ with $z = 6$, wherefore $f = 0.75$, which makes the triangular lattice a promising candidate to find kinetically frustrated ferromagnetism. The associated (single-particle) density of states $D(E)$ can be computed analytically in terms of a complete elliptic integral of the first kind and exhibits a van Hove singularity at an energy $E = -2t$, corresponding to a density of 1.5 electrons per site; we therefore set $\delta = 0.5$ to

maximize the density of states at the Fermi level.

Remarkably, at $U/t = 10$, we see clear evidence of a ferromagnetic ground state, as exemplified by Fig. 5(b) for a 8×4 cylinder, whereas at $U/t = 4$, we find a state with stripelike correlations in the spin density [Fig. 5(a)]. To eliminate the possibility of strong finite-size effects, we consider two different cylinders with one being double the size of the other. In both cases, we see that the nearest-neighbor radial correlator C_a attains its maximum possible value by $U/t \simeq 11$ although the onset of ferromagnetic correlations can already be seen for much lower $U/t \sim 6$. We emphasize that this observed ferromagnetism is truly a many-body phenomenon of the Nagaoka type, as opposed to Stoner ferromagnetism, which occurs whenever $D(E_F)U > 1$ and should thus set in for infinitesimal $U/t > 0$.

Discussion and outlook.—Despite the prediction of Nagaoka ferromagnetism more than half a century ago, its actual realization has proved considerably more challenging. This may partially be attributed to the fragility of the Nagaoka state itself, which was theorized for an infinite system doped with exactly one hole at $U/t = \infty$. In this work, we address a central question: moving away from such an idealized limit, can ferromagnetism occur for finite U/t and macroscopic dopings? Using large-scale DMRG computations, we reveal robust ferromagnetism in a generalized Hubbard model, analyze its origins, and explore its intimate connections to the underlying lattice geometry. Given that half-filled Hubbard systems are generically either antiferromagnetic (when on a bipartite lattice) or paramagnetic, the emergence of ferromagnetism is indeed a beautiful demonstration of the surprises that strong correlations may engender.

The rarity of Nagaoka ferromagnetism in conventional solid-state materials is well documented. For instance, in many candidate Mott-insulator oxides and chalcogenide

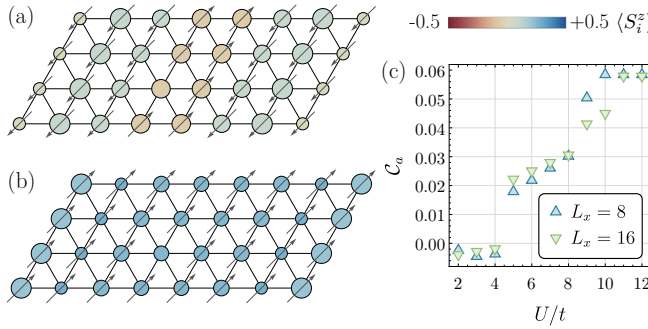


Figure 5. (a) Ground states of the Hubbard model ($\tilde{t} = t$) on a triangular lattice for (a) $U/t = 4$ and (b) $U/t = 10$, exhibiting striped and ferromagnetic correlations, respectively. (c) The nearest-neighbor correlator C_a , plotted here for two width-4 cylinders of different lengths, shows that the Nagaoka state is realized for moderate U/t even for large system sizes.

systems, U/t is insufficient to generate ferromagnetism. Likewise, strong positional disorder present in doped semiconductors often localizes mobile carriers and inhibits ferromagnetism [30, 58]. Optical lattice platforms, on the other hand, offer clean and tunable alternatives to circumvent these issues. In such systems, the lattice depth can be varied to control the tunnelings t, \tilde{t} while the ratio U/t can be independently tuned via a Feshbach resonance [59]. Moreover, one can use the naturally arising [60] density-dependent tunnelings [61] for the straightforward implementation of our extended model (1), thereby paving a new route to obtaining the Nagaoka state.

Even without any such modifications, our results for the case of $\tilde{t} = t$ directly apply to the recent experiments of Ref. 33, which probe a square-lattice Hubbard model with a next-nearest-neighbor hopping of strength t' . In the limit $t \approx t'$ (when the square lattice is reconstructed to a triangular one), Xu *et al.* [33] observe signatures of ferromagnetic correlations for $U/t \approx 9$ with $\delta \approx 0.5$. This is in excellent agreement with our predictions in Fig. 5, thus highlighting the geometric frustration of the kinetic energy as a mechanism for the experimentally observed ferromagnetism.

We thank E. M. Stoudenmire, W. S. Bakr, and M. L. Prichard for useful discussions. The computations in this paper were performed using the ITensor library [62]. R.S. is supported by the Princeton Quantum Initiative Fellowship. R.N.B. acknowledges support from the UK Foundation at Princeton University and thanks the Aspen Center for Physics, where some of the ideas were conceptualized, for hospitality.

F.-M. Le Régent, A. Kirsch, Y. Wang, A. J. Kim, E. Kozik, E. A. Stepanov, A. Kauch, S. Andergassen, P. Hansmann, D. Rohe, Y. M. Vilk, J. P. F. LeBlanc, S. Zhang, A.-M. S. Tremblay, M. Ferrero, O. Parcollet, and A. Georges, *Phys. Rev. X* **11**, 011058 (2021).

- [3] M. Qin, T. Schäfer, S. Andergassen, P. Corboz, and E. Gull, *Annu. Rev. Condens. Matter Phys.* **13**, 275 (2022).
- [4] P. A. Lee, N. Nagaosa, and X.-G. Wen, *Rev. Mod. Phys.* **78**, 17 (2006).
- [5] T. Esslinger, *Annu. Rev. Condens. Matter Phys.* **1**, 129 (2010).
- [6] L. Tarruell and L. Sanchez-Palencia, *C. R. Phys.* **19**, 365 (2018).
- [7] L. W. Cheuk, M. A. Nichols, K. R. Lawrence, M. Okan, H. Zhang, E. Khatami, N. Trivedi, T. Paiva, M. Rigol, and M. W. Zwierlein, *Science* **353**, 1260 (2016).
- [8] M. F. Parsons, A. Mazurenko, C. S. Chiu, G. Ji, D. Greif, and M. Greiner, *Science* **353**, 1253 (2016).
- [9] J. H. Drewes, L. A. Miller, E. Cocchi, C. F. Chan, N. Wurz, M. Gall, D. Pertot, F. Brennecke, and M. Köhl, *Phys. Rev. Lett.* **118**, 170401 (2017).
- [10] A. Mazurenko, C. S. Chiu, G. Ji, M. F. Parsons, M. Kanász-Nagy, R. Schmidt, F. Grusdt, E. Demler, D. Greif, and M. Greiner, *Nature* **545**, 462 (2017).
- [11] B. M. Spar, E. Guardado-Sánchez, S. Chi, Z. Z. Yan, and W. S. Bakr, *Phys. Rev. Lett.* **128**, 223202 (2022).
- [12] E. Manousakis, *Rev. Mod. Phys.* **63**, 1 (1991).
- [13] K. A. Chao, J. Spalek, and A. M. Oleś, *Phys. Rev. B* **18**, 3453 (1978).
- [14] P. W. Anderson, *Phys. Rev.* **115**, 2 (1959).
- [15] Y. Nagaoka, *Phys. Rev.* **147**, 392 (1966).
- [16] G.-s. Tian, *J. Phys. A: Math. Gen.* **23**, 2231 (1990).
- [17] A. Sütő, *Commun. Math. Phys.* **140**, 43 (1991).
- [18] T. Hanisch and E. Müller-Hartmann, *Ann. Phys. (Berl.)* **505**, 381 (1993).
- [19] T. Hanisch, B. Kleine, A. Ritzl, and E. Müller-Hartmann, *Ann. Phys. (Berl.)* **507**, 303 (1995).
- [20] P. Wurth, G. Uhrig, and E. Müller-Hartmann, *Ann. Phys. (Berl.)* **508**, 148 (1996).
- [21] B. Doucot and X. G. Wen, *Phys. Rev. B* **40**, 2719 (1989).
- [22] Y. Fang, A. E. Ruckenstein, E. Dagotto, and S. Schmitt-Rink, *Phys. Rev. B* **40**, 7406 (1989).
- [23] B. S. Shastry, H. R. Krishnamurthy, and P. W. Anderson, *Phys. Rev. B* **41**, 2375 (1990).
- [24] A. G. Basile and V. Elser, *Phys. Rev. B* **41**, 4842 (1990).
- [25] A. Barbieri, J. A. Riera, and A. P. Young, *Phys. Rev. B* **41**, 11697 (1990).
- [26] R. Strack and D. Vollhardt, *J. Low Temp. Phys.* **99**, 385 (1995).
- [27] H. Tasaki, *Prog. Theor. Phys.* **99**, 489 (1998).
- [28] D. Vollhardt, N. Blümer, K. Held, M. Kollar, J. Schlipf, M. Ulmke, and J. Wahle, in *Advances in Solid State Physics* **38** (Springer, 1999) pp. 383–396.
- [29] E. Nielsen and R. N. Bhatt, *Phys. Rev. B* **76**, 161202 (2007).
- [30] E. Nielsen and R. N. Bhatt, *Phys. Rev. B* **82**, 195117 (2010).
- [31] Diluted magnetic semiconductors can also exhibit similar ferromagnetism; R. N. Bhatt and X. Wan, *Int. J. Mod. Phys. C* **10**, 1459 (1999); M. Berciu and R. N. Bhatt, *Phys. Rev. Lett.* **87**, 107203 (2001); R. N. Bhatt, M. Berciu, M. P. Kennett, and X. Wan, *J. Supercond.* **15**, 71 (2002).

- [1] D. P. Arovas, E. Berg, S. A. Kivelson, and S. Raghu, *Annu. Rev. Condens. Matter Phys.* **13**, 239 (2022).
- [2] T. Schäfer, N. Wentzell, F. Šimkovic, Y.-Y. He, C. Hille, M. Klett, C. J. Eckhardt, B. Arzhantsev, V. Harkov,

[32] S. R. White, *Phys. Rev. Lett.* **69**, 2863 (1992); *Phys. Rev. B* **48**, 10345 (1993); U. Schollwöck, *Rev. Mod. Phys.* **77**, 259 (2005); *Ann. Phys.* **326**, 96 (2011).

[33] M. Xu, L. H. Kendrick, A. Kale, Y. Gang, G. Ji, R. T. Scalettar, M. Lebrat, and M. Greiner, [arXiv:2212.13983 \[cond-mat.quant-gas\]](https://arxiv.org/abs/2212.13983) (2022).

[34] E. M. Stoudenmire and S. R. White, *Annu. Rev. Condens. Matter Phys.* **3**, 111 (2012).

[35] J. Zaanen and O. Gunnarsson, *Phys. Rev. B* **40**, 7391 (1989).

[36] K. Machida, *Physica C Supercond.* **158**, 192 (1989).

[37] M. Kato, K. Machida, H. Nakanishi, and M. Fujita, *J. Phys. Soc. Jpn.* **59**, 1047 (1990).

[38] J. M. Tranquada, B. J. Sternlieb, J. D. Axe, Y. Nakamura, and S.-i. Uchida, *Nature* **375**, 561 (1995).

[39] M. Vojta, *Adv. Phys.* **58**, 699 (2009).

[40] S. R. White and D. J. Scalapino, *Phys. Rev. Lett.* **80**, 1272 (1998).

[41] S. R. White and D. J. Scalapino, *Phys. Rev. Lett.* **91**, 136403 (2003).

[42] G. Hager, G. Wellein, E. Jeckelmann, and H. Fehske, *Phys. Rev. B* **71**, 075108 (2005).

[43] C.-C. Chang and S. Zhang, *Phys. Rev. Lett.* **104**, 116402 (2010).

[44] B.-X. Zheng, C.-M. Chung, P. Corboz, G. Ehlers, M.-P. Qin, R. M. Noack, H. Shi, S. R. White, S. Zhang, and G. K.-L. Chan, *Science* **358**, 1155 (2017).

[45] E. W. Huang, C. B. Mendl, S. Liu, S. Johnston, H.-C. Jiang, B. Moritz, and T. P. Devereaux, *Science* **358**, 1161 (2017).

[46] E. W. Huang, C. B. Mendl, H.-C. Jiang, B. Moritz, and T. P. Devereaux, *npj Quant. Mater.* **3**, 22 (2018).

[47] A. S. Darmawan, Y. Nomura, Y. Yamaji, and M. Imada, *Phys. Rev. B* **98**, 205132 (2018).

[48] L. F. Tocchio, A. Montorsi, and F. Becca, *SciPost Phys.* **7**, 021 (2019).

[49] A. Wietek, Y.-Y. He, S. R. White, A. Georges, and E. M. Stoudenmire, *Phys. Rev. X* **11**, 031007 (2021).

[50] The collapse of the data for the two largest system sizes atop one another suggests that our observations are free of finite-size effects along the axial dimension.

[51] D. C. Mattis, *The Theory of Magnetism I*, Springer Series in Solid-State Sciences (Springer Berlin, Heidelberg, 1981).

[52] J. Merino, B. J. Powell, and R. H. McKenzie, *Phys. Rev. B* **73**, 235107 (2006).

[53] G. M. Pastor, R. Hirsch, and B. Mühlischlegel, *Phys. Rev. Lett.* **72**, 3879 (1994).

[54] G. M. Pastor, R. Hirsch, and B. Mühlischlegel, *Phys. Rev. B* **53**, 10382 (1996).

[55] T. Hanisch, G. S. Uhrig, and E. Müller-Hartmann, *Phys. Rev. B* **56**, 13960 (1997).

[56] J. O. Haerter and B. S. Shastry, *Phys. Rev. Lett.* **95**, 087202 (2005).

[57] W. Barford and J. H. Kim, *Phys. Rev. B* **43**, 559 (1991).

[58] R. N. Bhatt and P. A. Lee, *Phys. Rev. Lett.* **48**, 344 (1982).

[59] C. Chin, R. Grimm, P. Julienne, and E. Tiesinga, *Rev. Mod. Phys.* **82**, 1225 (2010).

[60] J. C. Amadon and J. E. Hirsch, *Phys. Rev. B* **54**, 6364 (1996).

[61] O. Dutta, M. Gajda, P. Hauke, M. Lewenstein, D.-S. Lühmann, B. A. Malomed, T. Sowiński, and J. Zdziarski, *Rep. Prog. Phys.* **78**, 066001 (2015).

[62] M. Fishman, S. R. White, and E. M. Stoudenmire, *SciPost Phys. Codebases* , 4 (2022).